Indian Journal of Engineering & Materials Sciences
Vol. 15, April 2008, pp. 126-132

Low temperature ferroelectric behaviour of PVDF based composites

Namrata Shukla, Archana Shukla, Awalendra K Thakur* & R N P Choudhary
Department of Physics & Meteorology, Indian Institute of Technology, Kharagpur 721 302, India

Received 9 December 2006; accepted 28 February 2008

A polymer nanocomposite based on poly (vinylidenefluoride) (PVDF) and unmodified montmorillonite clay has been studied for structural phase transformation, ferroelectric and piezoelectric properties. The effect of clay concentration in modifying PVDF crystalline phase structure has been substantial leading to α→β phase transformation in PVDF. This aspect has been confirmed through X-ray diffraction and infrared spectroscopy data. The effect of structural change has been clearly observed in inducing dipolar characteristics in PVDF matrix supported by changes in dielectric permittivity variation as a function of temperature and frequency. A close resemblance in the permittivity and loss tangent peak position as a function of temperature has been correlated with dipolar ordering in PVDF matrix induced by clay. However, this ordering depends on clay concentration. The clay induced dipolar ordering is also supported by piezoelectric coefficient measured for various compositions of clay.

Coexistence of ferroelectric, piezoelectric and piezoelectric properties in the materials system under ambient conditions has always been desirable goal to be achieved. A polar polymeric system, keeping this objective in mind, has always an edge over ceramics in view of tensile properties dimensional flexibility, mould ability of shape and size large strain without structural fatigue light weight and low cost. Poly (vinylidene fluoride) (PVDF) having chemical structure $[-(CF_2-CH_2)_n-]$ has been a traditional polar polymer exhibiting piezoelectric, pyroelectric and ferroelectric characteristics. The location of H- atom and F-atom along the polymer chain of PVDF creates a unique dipolar effect that in turn modulates its properties such as the solubility, crystal morphology, dielectric constant to an unusually high value of 12 (i.e., 4 times the value of reported normally for polymers), lower signal-to-noise ratio and improved electromechanical response. Further, a low glass transition temperature (i.e. –35°C) imparts PVDF a flexible backbone capable of being strained at room temperature.

The origin of ferro, pyro, and piezo properties in PVDF lies in its internal crystal structure imparting a net non-zero dipole moment due to high electro-negativity of F-atom and orientation of crystallite dipoles in a preferred direction. Since, PVDF has applicability high crystallinity (~50-60%), the dipole arising from all crystallites are most likely to take a preferred orientation in the presence of an external applied field imparting it unusually high permittivity among polymers. In view of this, PVDF has been studied extensively for its pyro, piezo electro-optic and electro-mechanical characteristics since 1969[1-3]. These properties of PVDF are very useful for device applications such as ultrasound, transducers, medical diagnosis/non destructive evaluation and large scale integration of electronic circuits[4-6].

However, the properties of polymorphism exhibited by semi-crystalline PVDF resulting in 5 different structural forms (namely α, γ, β, σ & ε)and each crystal phase having different molecular confirmation affects its dipolar characteristics due to preferential orientation of atomic groups around carbon atom[7,8] and packing of polymer chain into crystal. When polymer chain packing in the unit cell occur in such a way that the dipoles attributed to each crystallite align parallel to one another, a non-zero dipole moment result as in the case of β-, γ-, σ-crystal phases which are polar. On the other hand when the polymer chain packing in the unit cell assumes antiparallel alignment of molecular dipoles, net dipole moments in the crystal become zeroes in the case of non-polar α, and ε phases of PVDF. Among these polymorphic forms three important crystalline forms of PVDF are; β (orthorhombic), α (pseudo- orthorhombic) and γ (monoclinic) having chain confirmations TTTT, TGTGTG and TTTGTTTG respectively[9,10]. The α phase in the most commonly available form in pristine PVDF whereas the β phase has strong C-F polar bond with the highest dipole moment (7×10^{-30}C.m) per unit in contrast to the normal C-F

*For correspondence (E-mail: akt@phy.iitkgp.ernet.in)

bond dipole moment (6.4×10^{-30}C.m)[11]. So, structurally the β phase is expected to exhibit stronger ferro-, piezo and pyro electric properties in comparison to other structural phases of PVDF.

As a result there has been exhaustive research to transform the commonly available isotropic α phase PVDF in to its highly oriented β phase in view of its technological significance. Various approaches to achieve this such as poling under influence of an external electric field[12-14], mechanical deformation (uniaxial/biaxial drawing) under controlled conditions of high pressure and temperature[15,16], thermal treatment/annealing[17], crystal structure from melt prepared in various polar solvents such as cyclo-hexanone[18], dimethyl sulphoxide[19] and use of γ radiation at very high radiation dose (500 Mrad)[20] has been used previously. All such approach to realize α→β transition in PVDF are very meticulous and require in most of the cases extreme experimental conditions to be maintained for obtaining the β polymorph. Further, complete α→β transition has never been obtained respective of the procedure adopted.

Recently, a new approach of polymer nanocomposite formation using unmodified/modified nano clay has begun since 2002 onwards[21-25]. Although, there has been a significant disagreement on the mechanism of nanocomposite formation in these new reports, α→β phase conversion appear to have been realized with β phase stabilization via van der walls interaction in the clay layers, chain length distribution desirable for improvement in the electrical properties of PVDF. This paper aims to report a PVDF – clay nanocomposite with higher clay concentration (upto ~15 wt%). The effect of clay concentration on structural, micro-structural properties has been investigated and its co-relation with ferroelectric, piezoelectric properties has been studied.

Experimental Procedure

Polymer nanocomposite films with various clay concentrations (0%, 2%, 10%, 15%) based on poly vinylidene fluoride (PVDF) and unmodified sodium montmorillonite clay. An appropriate stoichiometric ratio of PVDF (1 g) and various weight fractions of clay (w.r.t. polymer weight) were taken and dissolved in acetone (Merck) and the solution was stirred for 12 h. The resulting final polymer solutions for each clay concentration have been casted in poly propylene dishes and the solvent was allowed to evaporate slowly at room temperature (27°C) Finally free standing polymer clay nanocomposite films were obtained dried at 40°C to remove residual solvent if and stored in an inert medium for further analysis.

The X-ray pattern were recorded at room temp using a diffractometer (X'Pert Pro PW 3040/60) with Cu-K_α radiation (λ=1.5406Å) over a range of 2θ =10-60° at a scan rate ~4°/min. The surface morphology with the variation in clay concentration was studied by scanning electron microscopy (SEM Model no AMSCAN-2 JEOL). Fourier transformed infrared spectrum (FTIR) data were collected in the mid-frequency range (4000-400 cm^{-1}) at a scan rate of 32 with spectral resolution of 4 cm^{-1} using Thermo Nicolet Spectrophotometer (Model: NEXUS –870). The dielectric measurements on the composite films were carried using a computer interfaced impedance analyzer (HIOKI LCR Hi-Tester Model 3532, Japan) in the frequency range of 0.1 Hz-100 kHz over a range of temperature (200-450 K) and cell configuration used for dielectric measurement SS │PNC │SS (SS stands for stain less steel blocking electrode and PNC is for polymer-nanocomposite film for various clay concentration). For all the measurements the a.c. input signal of 200 mV is applied across the cell. The dielectric function (permittivity and tangent loss factor) has been observed as a function of temperature and frequency. The piezoelectric constants of the composite films were carried out using a peizometer system (PM 200).

Results and Discussion

X-ray diffraction (XRD) analysis

X-ray diffraction (XRD) studies have been carried out to confirm the changes occurring in the crystalline phase characteristics of the PVDF on addition of unmodified montmorillonite clay (having nanometric channels dipolar with groups and water of crystallization**)** into the polymer matrix. Figure 1(a-d) shows XRD pattern of PVDF-Montmorillonite clay for various clay concentrations up to 15 wt% w.r.t polymer host (PVDF). The diffraction pattern of pure PVDF (Fig. 1a) shows reflections of predominantly α-phase occurring at 18.9° (0.48 nm), 20.35° (0.44 nm), 26.9° (0.32 nm) and 36.2° (0.24 nm) that has been indexed to 020,110,120 and 002 crystal planes. In addition, a number of weak shoulders lying on primary peaks appear at 2θ ~ 17.8° (100), 20.9° (011), 27.2° (021) and 27.6° (111). These shoulders have also been attributed to the α-crystalline phase of the PVDF. Some additional reflections in the XRD

pattern, over and above those of the α-phase of PVDF, also appears at 20.7° (110/200), 41° (201/111), 43° (220), 52° and 56.2°. These peaks have been attributed to the presence of polar β-phase in the polymer matrix. The peaks at 52° and 56.2° could not be indexed and may be related to a possible α→β phase transition of PVDF film obtained from the solution crystallization under controlled conditions and appears to be consistent with the previous reports[26,27].

A clear modification in the diffraction pattern has been observed on clay addition into the PVDF matrix .The characteristic β-phase reflection attributed to the plane 110/200 appears at 2θ ~ 20.7°. In addition, the intensity of the β-phase peaks observed at 41°, 43°, 52° and 56.2° increases with increasing concentration of the unmodified montmorillonite clay. On the other hand, a comparative decrease in the intensity and increase in the width of the characteristic α-phase peak (110) has been recorded on nanoclay addition.

But the *d*-spacing of this peak does not change. These evidences suggest that polymer-nanoclay composite formation has resulted in α→β phase transition in PVDF and both the α and β phases are coexisting. The minimum energy (i.e ~330 cal/mol) required for such a transition to occur as predicted by molecular dynamic simulation studies[28] is provided by

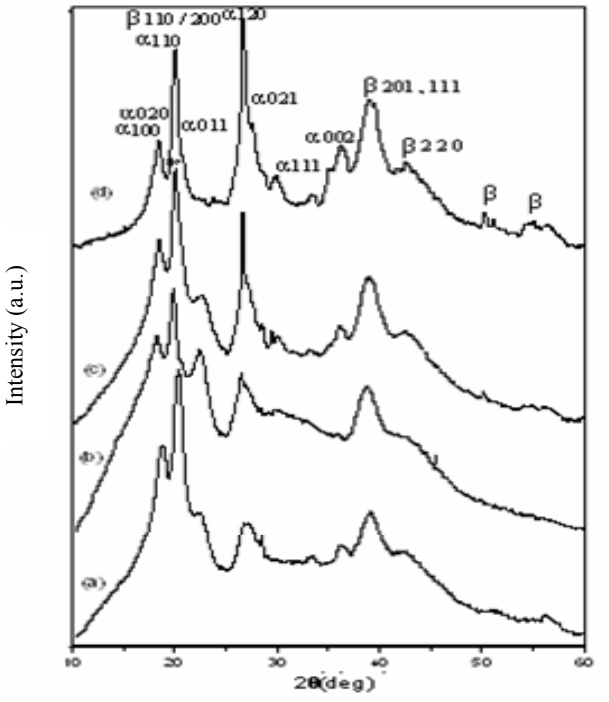

Fig. 1 — X-ray diffraction pattern of polyvinylidenefluoride (PVDF)–montmorrilonite clay nanocomposite for various clay concentrations: (a) 0% clay, (b) 2% clay,, (c) 10% and (d) 15% clay

interaction of PVDF chain with silicate layer of the clay via short-range Vander Walls interaction. However, a possibility of such an interaction remains to be seen in the experimental results such as infrared spectrum corroborating evidence for the same.

Fourier transform infrared (FTIR) spectrum

Figure 2(a-e) shows FTIR spectrum of PVDF – nanoclay composites for different clay concentration. The FTIR spectrum of pure PVDF and unmodified clay has also been shown for comparison. The characteristic band pattern of polymer host (PVDF), clay (montmoillonite) has been noted and recorded, and the vibrations/modes associated with each group in the system have been assigned (Table 1). The spectrum on comparison, reveals clay peaks appearing separately (marked-↓) for higher concentration of clay. This suggests composite formation. The bands attributed to clay and PVDF phases have been identified and recorded in Table 1.

The addition of clay into PVDF matrix has caused significant changes in the spectral pattern visible very clearly in the wave number region 532, 975 and 1000-1400 cm^{-1}. A clear interaction between PVDF matrix and silicate layer of clay is evidenced indicated by changes in 525 cm^{-1} clay band and attributed to ν_s[Al (Mg)-O-Si] and 532 cm^{-1} band of PVDF attributed to bending mode of CF_2. A shift in this band occurs towards the lower wave number side (532→529) with increasing clay concentration. This may be related to a change in the chemical environment of CF_2 group

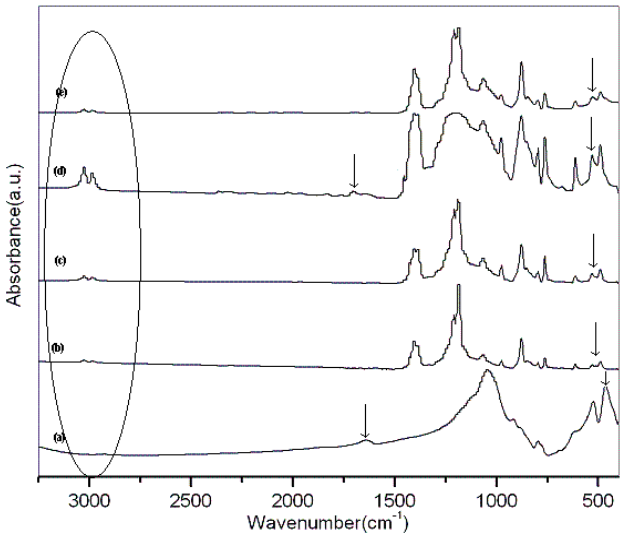

Fig. 2 — Fourier transform infrared spectrum of PVDF–nanoclay composites for various clay concentrations: (a) montmorillonite clay, (b) PVDF, (c) 2% clay, (d) 10% clay and (e) 15% clay

Table 1— FTIR band assignment for PVDF–clay nanocomposite films

Unmodified NaMMT	PVDF PURE	PVDF (2%Clay)	PVDF (10%Clay)	PVDF (15%clay)	Group	Source
465				465	ν_s (Al (Mg)-O-Si	clay
	489.67	490.02	489.76	488	CF_2 bending &waging	α phase(PVDF)
525					ν_a(Al (Mg)-O-Si	clay
	532	530	529	529	CF_2 bending	α phase(PVDF)
	614	612	614	613	CF_2 bending &skeletal bending of C(F)- C(H)-C(F)	α phase(PVDF)
	762	762	762	762	skeletal bending of C(F)- C(H)-C(F)	α phase(PVDF)
797					ν (Al (Mg)-O	clay
	796	796	796	797	CH_2 Rocking	α phase(PVDF)
	840	841	841	841	CH_2 Rocking & CF_2 asymmetry. stretching	β phase(PVDF)
	853	854	854	850	γ (C-H $_2$)	α phase(PVDF)
	877.65	877.54	878	877	CH $_2$ Rocking	α phase(PVDF)
	975	975	977	977	t(CH_2)	α phase(PVDF)
1045					ν (Si –O)	clay
	1067	1066	1066	1064	ν_s (C-C) + ωCF2 + ω (CH2)	β phase(PVDF)
	1183	1185	1185	1185	ν_s (CF2) – γ(CF2) + γ (CH2)	β phase(PVDF)
	1210	1211	1212	1210	t (CH2)	β phase(PVDF)
	1383.	1385.	1385	1385	δ (CH_2) + ω (CH_2)	β phase(PVDF)
	1404	1404	1404	1403	ω(CH_2)+ ν_{as}(C-C)	β phase(PVDF)

with silicate group on the clay possibly by short range Vander Walls interaction. Another change in band position with a shift towards higher side of wave number scale has been noticed for twisting vibrational mode [τ{CH_2}] of PVDF appearing at 975 cm^{-1}. This band shifts to a new position at 977 cm^{-1} for 10% clay onwards. The twisting in CH_2 group may be related to a possible change in conformation of PVDF chain due to strong interaction between the silicate layer and the most electronegative F-atom of CF_2 group in the chain. Such a possibility is also suggested by a shift in γ-(CH_2) + ν_{as}(CF_2) vibrational mode towards higher wave number (840-841 cm^{-1}) on clay addition. A higher shift indicates stiffening of the polymer back bone which is expected on change in conformation and on twisting in the polymer chain. The spectral band region 1000-1400 cm^{-1} has shown significant changes in its pattern with increasing clay concentration. The changes occurring in this region have been recorded for PVDF bands occurring at 1067, 1183, 1210 and 1383 $cm^{-1.}$ They have been attributed to coupled oscillations of the C-C, CF_2 and CH_2 groups of the polymer chain and their exact assignment is given in the Table 1 along with their association with the β crystal phase of PVDF. This seems logical as the coupled oscillation mode attributed to ν_s (C-C) –γ(CF_2) + ω(CH_2) shows a lower shift permitting a change in conformation on the clay addition due to interaction between polymer CF_2 chain and clay silicate layer. This is followed by an upward shift of all subsequent bands appearing at 1183, 1210, 1383 cm^{-1} with the increasing clay concentration. The ultimate result is stiffening of polymer chain on change in group location around C–C band in the chain. Further, the changes occurring at 2983 cm^{-1} and 3024 cm^{-1} with clear splitting in the band corroborates strong interaction between PVDF-clay in the composite films. The overall effect is a change in the crystalline order in the PVDF matrix on nanocomposite formation with various concentration of nanoclay suggesting a feasibility of α→β transition. These observations are in the good agreement with the XRD results.

Scanning electron micrograph (SEM) analysis

Figure 3 (a-d) shows the scanning electron micrographs for the various clay concentrations. It shows a clear modulation of PVDF microstructure and phase characteristics on nanocomposite formation. PVDF film micrograph (Fig. 3a) exhibits small crystallites with heterogeneous distribution in the matrix. The crystalline domains comprise of crystallite having average dimension ~ 2-3 μm. A lamellar distribution of crystalline domain with traces of two polymorphic phases (α & β) observed for pure PVDF. The PVDF microstructure gets drastically

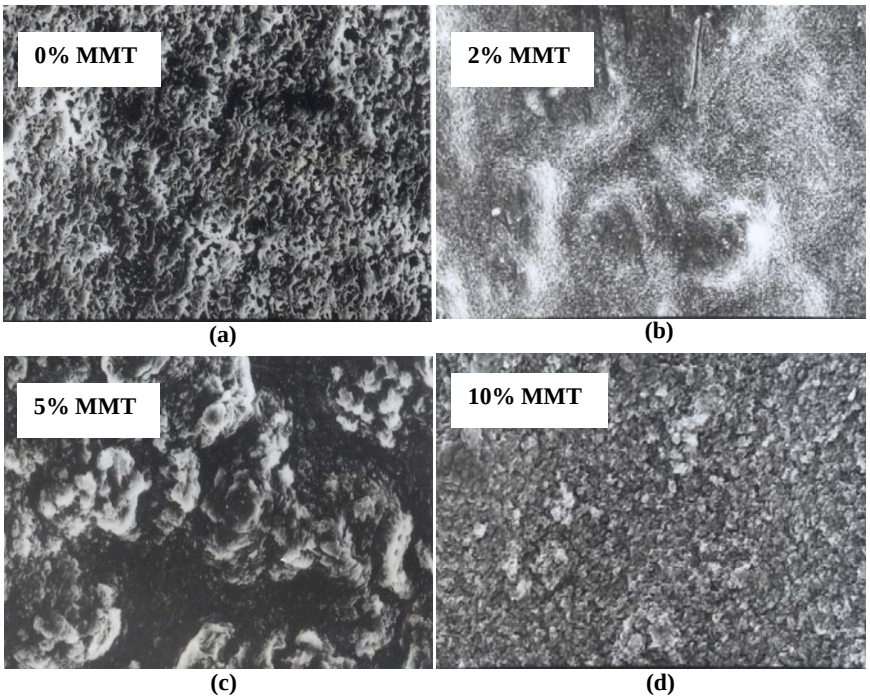

Fig. 3 — SEM micrographs of PVDF-clay composite films: (a) 0% clay, (b) 2% clay, (c) 5% clay and (d) 15% clay

modified on clay addition [Fig. 3(b-c)] which becomes more prominent with increasing clay concentration (2-15%) suggesting an effective role played by the nanoclay as a nucleating agent resulting in the changes in polymer film morphology. It shows a bimodal morphology with modified crystalline domain having average crystallite size of the order of 40-50 μm. The presence of two distinct crystalline phases in all nanocomposite films attributed to α and β-crystal phases are clearly visible. The results are in good agreement with the XRD and FTIR observations.

Dielectric analysis

The variation of dielectric properties (permittivity and loss factor) as a function of temperature has been performed on PVDF–nanoclay based nanocomposite polymer films to evaluate the effect of clay concentration on polymer-chain orientation and its dipolar characteristics.

Figure 4(a-d) shows the variation of dielectric permittivity as a function of temperature at different frequencies (1 kHz, 10 kHz, and 100 kHz) for various clay concentration in the nanocomposite films.

The ε_r versus T pattern for pure PVDF (Fig. 4a) shows a small hump at 250 K (very near to glass transition temperature) of the polymer host. This may be related to the β relaxation in the PVDF attributed to trans-conformation in its polar crystalline phase. As

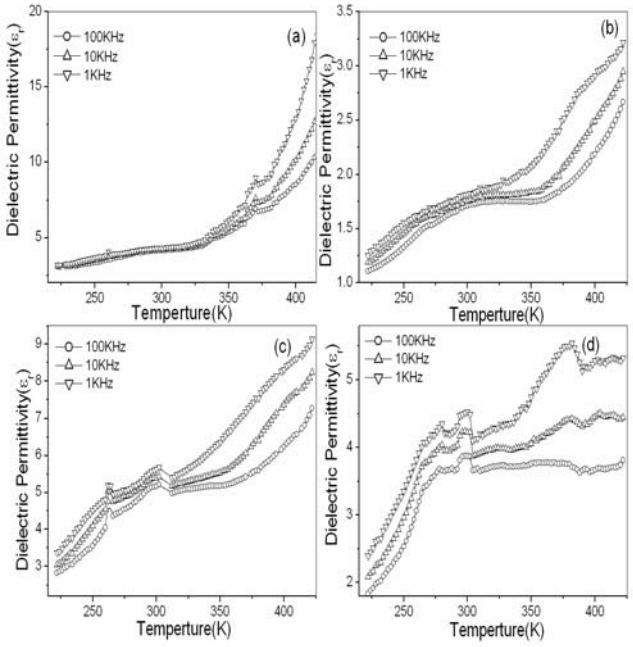

Fig. 4 — Variation of dielectric permittivity (ε_r) of PVDF-nanoclay composite films as a function of temperature with varying clay concentration: (a) pure PVDF (b) 2% clay, (c) 10% clay and (d) 15% clay

the temperature is increased, another small maximum becomes noticeable for pure PVDF sample irrespective of frequency at T = 370 K well below its crystalline melting temperature. It has been related to α relaxation in the literature[16]. However, a

contribution due to the orientational correlation of the moments in the crystalline phase arising due to β crystalline phase cannot be ruled out. It seems logical in view of a direct correlation with the variation of loss tangent (tanδ) as a function of temperature showing two small maximum at $T \sim 250$ K and 370 K irrespective of maximum in both the ε_r versus T and tanδ versus T plot for pure PVDF at nearly the same temperature. This indicates the possibility of dipolar ordering under thermal activation and may be attributed to the ferro- to para-electric phase transition in the material in its crystalline region. Such a transition is feasible normally in the β crystalline phase and it seems feasible in the light of FTIR and XRD results in the present investigation.

The variation in the pattern of ε_r versus T and tanδ versus T appears to be affected strongly on the composite formation with the nanoclay. The presence of peaks in both the plots as shown in Figs 4(c-d) and 5(c-d) becomes more prominent with the increasing clay concentration having the common feature that the peaks in both permittivity and loss pattern almost coincide on temperature scale. The only difference in the variation pattern in comparison with pure PVDF (Figs 4a and 5a) is that both the permittivity and loss peaks shift towards lower side on the temperature scale, the shift being more pronounced for the second peak (370 K→300 K in the permittivity peak and 375 K→340 K in the loss peak) with the increasing clay concentration in the PVDF matrix. The observation may be related to a better dipolar ordering at a relatively lower temperature in the PVDF-nanoclay based nanocomposite films and can be attributed to an enhanced β-crystal phase in the PVDF matrix on nanocomposite formation. Evidences in support of this possibility has been recorded in XRD and FTIR results where the number of peaks attributed to β-crystal phase in both the pattern was more and that too with enhanced intensity on nanocomposite formation. The variation of dielectric permittivity as a function of frequency at 302 K (room temperature) for pure PVDF and nanocomposite (10% clay concentration) is shown in Fig. 6. It shows low frequency dispersion and high frequency plateau with a clear indication of improvement in the dipolar features of composite films in comparison to that of pure PVDF. The low frequency dispersion may be related to the ionic species present in the matrix whereas the high frequency plateau region is attributed to orientational polarization of molecular dipoles. This contribution appears enhanced in nanocomposite films indicated by a higher value of permittivity in the plateau region for PVDF – 10% clay based films.

The frequency dependence of permittivity can be fitted to the equation:

$$\varepsilon(\omega) = \varepsilon_\infty + BI_\omega(i\omega)^a \qquad \ldots(1)$$

where ε_∞ is static permittivity (high frequency saturation limit of the real part of the permittivity) of the non-conductive phase, B and a are constants. The

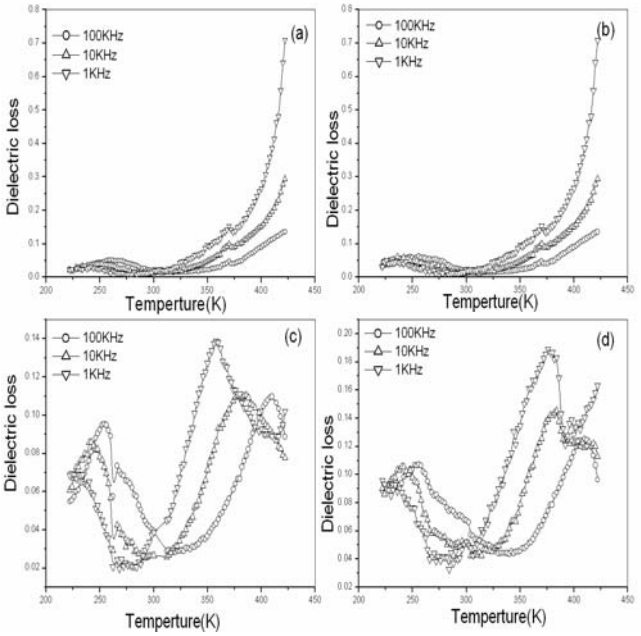

Fig. 5 — Variation of dielectric loss of PVDF-nanoclay composite films as a function of temperature with varying clay concentrations: (a) pure PVDF, (b) 2% clay, (c) 10% clay and (d) 15% clay

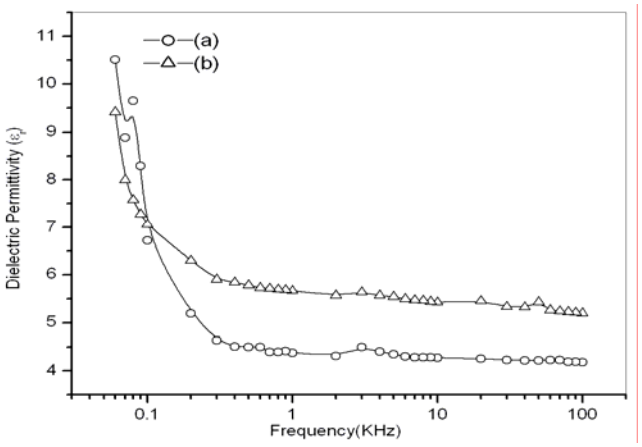

Fig. 6 — Variation of dielectric permittivity of PVDF-nanoclay composite films as a function of frequency with varying clay concentrations: (a) pure PVDF and (b) 10% clay

Table 2 — Piezoelectric Constant of PVDF and PVDF Clay Composites

Freq (Hz)	Piezoelectric constant d_{33} (pC/Newton)			
	Pure PVDF	PVDF + Clay 2%	PVDF + Clay 5%	PVDF + Clay 10%
110	6	9	15	—
150	2	6	9	12
200	1	4	6	10
250	1	3	6	7

value of ε_∞ is estimated to be approximately 4.5 and 6 for pure PVDF and 10% clay based nanocomposite films respectively suggesting an improved dipolar orderliness in the lattice. An improvement in dipolar characteristics of PVDF on nanocomposite formation attributed to $\alpha \rightarrow \beta$ phase transition has also been observed with an improvement in its piezoelectric coefficient on increasing clay concentration (Table 2).

Conclusions

A new approach for inducing structural phase transition from pristine α crystal phase of PVDF to β crystal phase has been attempted via nanocomposite formation of PVDF using nanoclay. XRD and FTIR data have confirmed α-β phase transition in PVDF. However, a complete phase conversion could not be achieved and the composite film comprises of both α and β phases with enhanced β phase fraction controlled by clay concentration. The enhancement in β phase has been reflected in terms of improved dipolar ordering in composite films when compared with pure PVDF. This has been indicated in the results of dielectric properties observed as a function of temperature as well as piezoelectric coefficient measurement.

References

1 Kawai H, *J Appl Phys*, 8(1969) 975-6.
2 Nalwa H S, *J Macro Mol SG*, C31 (1991) 341- 432.
3 Nalwa H S, Ed, *Ferroelectric polymers, Chemistry, Physics and Applications* (Marvel Dekker Inc.), 1995.
4 Inderherbergh J, *Ferroelectrics*, 115(4) (1991) 295-302.
5 Nagai M, Nakamura K, Uehara H, Kanamoto T, Takashi Y & Furukawa T, *J Polym Sci Pt B: Polym Phys*, 37(18) (1999) 2549-2556.
6 Stravshilov V L, *J Appl Phys*, 88(6) (2000) 3582-86.
7 Lovinger A J, *Science*, 220 (1983) 1115.
8 Briber R M & Khoury F, *J Polym Sci: Polym Phys*, 31 (1993) 1253.
9 Lovinger A J, *Macromolecules*, 14 (1981) 322.
10 Lovinger A J, *Macromolecules*, 15 (1982) 40.
11 Giannetti E, *Polymer Int*, 50(1) (2001) 10-26.
12 Lando J B, Olf H G, Peterlin A, *J Polym Sci,* A-1 (1966) 4:941
13 McGrath J C & Ward I M, *Polymer*, 21 (1980) 855.
14 Yun Ye, Yadong Jiang, Zhiming Wu, Hong Juan Zeng, Yajie Yang & Wei Li *Characterization and ferroelectric properties of Electric poled PVDF films*, *12th Int Symp on Electrets (ISE-12),* 2005.
15 Sajkiewicz P, Wasiak A & Goclowski Z, *Eur.Polym J*, 35 (1999) 423-29.
16 Barbosa R, Mendes J A, Sencadas V, Mano J F & Lanceros-Mendez S, *Ferroelectrics*, 294 (2003) 73-83.
17 Priya L & Jog J P, *J Polym Sci, Polym Phys*, 40 (2002) 1682.
18 Miller R L, *J Polym Sci, Pt B*, 14 (1976) 2325.
19 Toida Y & Chujo R, *Polym J*, 6 (1974) 191.
20 Galprin Y L & Kosmynin B P, *Vysokomol Soed*, A15 (1973) 2556.
21 Priya, L, Jog J P, *J Polym Sci, Polym, Phys*, 40 (2002) 1682.
22 Priya, L, Jog J P, *J Appl Polym Sci*, 89 (2003) 2036.
23 Liu H J, *J Polym Sci, Polym Chem*, 40 (2002) 3873.
24 Giannelis E P, Shah D, Maiti P, Gunn E, Schmitt D F & Jiang D D, *Adv Mater*, 16 (2004) 1173.
25 Pramoda K P, Mohammad A, Phang I.Y, Liu T, *Polym Int*, 54 (2005) 226.
26 Erizo Benedtti *et al*., *Polym Int*, 41 (1996) 35-41.
27 Douglas R Dillon *et al.*, *Polymer*, 47 (2006) 1678-1688.
28 Hasegawa R, Kobayashi M & Tadokoro H, *Polym J*, 3 (1972) 591-605.